

Effective Disruption of Phosphoprotein–Protein Surface Interaction Using Zn(II) Dipicolylamine-Based Artificial Receptors via Two-Point Interaction

Akio Ojida,[†] Masa-aki Inoue,[‡] Yasuko Mito-oka,[‡] Hiroshi Tsutsumi,[§]
Kazuki Sada,[‡] and Itaru Hamachi^{*,†,‡,§}

Contribution from the Department of Synthetic Chemistry and Biological Chemistry, Graduate School of Engineering, Kyoto University, Katsura, Kyoto, 615-8510, Japan, Department of Chemistry and Biochemistry, Graduate School of Engineering, Kyushu University, Fukuoka, 812-8581, Japan, and PRESTO (Organization and Function, JST)

Received October 1, 2005; E-mail: ihamachi@sbchem.kyoto-u.ac.jp

Abstract: Protein phosphorylation is ubiquitously involved in living cells, and it is one of the key events controlling protein–protein surface interactions, which are essential in signal transduction cascades. We now report that the small molecular receptors bearing binuclear Zn(II)-Dpa can strongly bind to a bis-phosphorylated peptide in a cross-linking manner under neutral aqueous conditions when the distance between the two Zn(II) centers can appropriately fit in that of the two phosphate groups of the phosphorylated peptide. The binding property was quantitatively determined by ITC (isothermal titration calorimetry), induced CD (circular dichroism), and NMR. On the basis of these findings, we demonstrated that these types of small molecules were able to effectively disrupt the phosphoprotein–protein interaction in a phosphorylated CTD peptide and the Pin1 WW domain, a phosphoprotein binding domain, at a micromolar level. The strategy based on a small molecular disruptor that directly interacts with phosphoprotein is unique and should be promising in developing a designer inhibitor for phosphoprotein–protein interaction.

Introduction

Protein–protein surface interactions play central roles in controlling numerous biological processes in living cells.^{1,2} A variety of specific protein complexes are formed in a time- and spatio-selective manner, producing the regulation and maintenance of complicated cellular events. Protein surface phosphorylation is, in particular, ubiquitously involved in signal transduction cascades and is controlled by phosphorylation–dephosphorylation processes catalyzed by the corresponding protein kinases and phosphatases.³ In many cases, the phosphorylation of certain protein surfaces by the upstream kinase creates a new binding site for the downstream proteins, in which the phosphorylated protein surface is recognized by a phosphoprotein binding domain such as the SH2, PTB, FHA, and WW domains.⁴ In general, these domains specifically interact with short peptide motifs containing phosphorylated amino acid residues (phospho-serine (pSer), -threonine (pThr), and -tyrosine (pTyr)), resulting in the recruitment of the phosphoprotein

involved in a signaling complex. A significant feature of these phosphoprotein–protein interactions is that the phosphate group on a protein–protein interface acts as a pinpoint residue crucial for the tight binding.⁵ That is, the phosphate group not only contributes to the high-affinity binding via salt bridges and/or hydrogen bonding but also induces the conformational rearrangement of surface amino acid residues necessary for the complementary interaction with the phosphoprotein binding domain. Thus, a small molecule that specifically interacts with the phosphate group on a protein surface may potentially disrupt the signaling complex and thus provide a potent modulator or disruptor for the signal transduction cascades.

Because of the biological significance of protein surface interactions, the design of small molecules that modulate or interfere with certain protein–protein interactions has been receiving considerable attention from the standpoint of fundamental molecular recognition^{6,7} and practical importance such as pharmaceutical applications.⁸ However, many protein–protein interfaces consist of a noncontinuous binding epitope on a relatively wide surface area (generally > 1100 Å²), which often makes it difficult to rationally design small molecule-based modulators or inhibitors. To date, much effort has also been

[†] Kyoto University.

[‡] Kyushu University.

[§] PRESTO.

(1) Giot, T.; et al. *Science* **2003**, *302*, 1727.

(2) (a) Ball, L. J.; Kühne, R.; Schneider-Mergener, J.; Oschkinat, H. *Angew. Chem., Int. Ed.* **2005**, *44*, 2852. (b) Pawson, T.; Nash, P. *Science* **2003**, *300*, 445. (c) Chakrabarti, P.; Janin, J. *Proteins* **2002**, *47*, 334. (d) Pawson, T.; Raina, M.; Nash, P. *FEBS Lett.* **2002**, *513*, 2.

(3) (a) Pawson, T.; Scott, J. D. *Trends Biochem. Sci.* **2005**, *30*, 286–290. (b) Johnson, S. A.; Hunter, T. *Nature Methods* **2005**, *2*, 17. (c) Sefton, B. M.; Hunter, T. *Protein Phosphorylation*; Academic Press: New York, 1998.

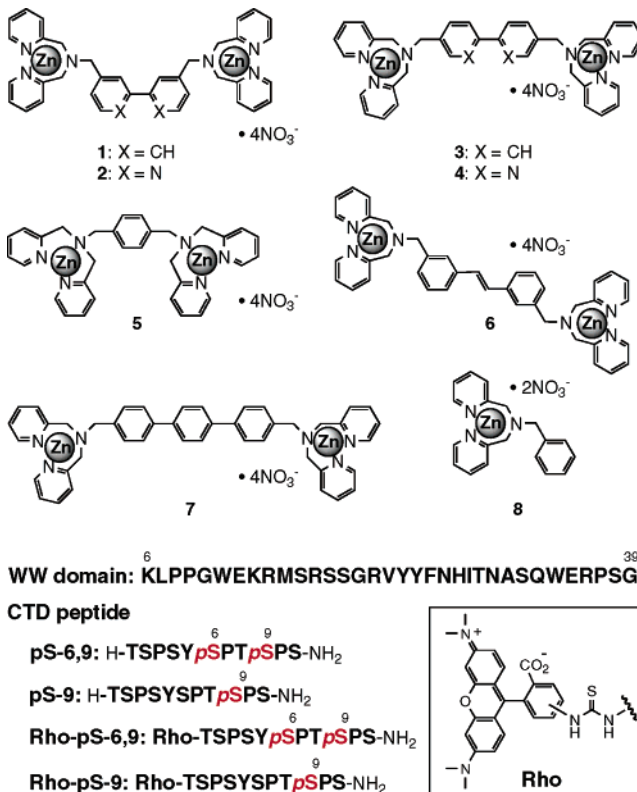
(4) (a) Yaffe, M. B. *Nat. Rev. Mol. Cell Biol.* **2002**, *3*, 177. (b) Yaffe, M. B.; Elia, A. *Curr. Opin. Cell Biol.* **2001**, *13*, 131. (c) Pawson, T.; Gish, G. D.; Nash, P. *Trends Cell Biol.* **2001**, *11*, 504. (d) Yan, K. S.; Kuti, M.; Zhou, M.-M. *FEBS Lett.* **2002**, *513*, 67. (e) Durocher, D.; Jackson, S. P. *FEBS Lett.* **2002**, *513*, 58. (f) Macias, M. J.; Wiesner, S.; Sudol, M. *FEBS Lett.* **2002**, *513*, 30.

(5) Johnson, L. N.; Lewis, R. J. *Chem. Rev.* **2001**, *101*, 2209.

devoted to the development of small molecular inhibitors for the surface interaction of the phosphoprotein binding domain such as the SH2 domain.⁹ Most of them are peptidemimetics of the phosphoprotein segment that can interact with a shallow surface pocket (surface groove) of the phosphoprotein binding domain. On the other hand, no small molecular inhibitors that directly interact with a phosphoprotein have yet been reported. This should be an alternative and promising strategy for developing unique inhibitors for these phosphoprotein–protein interactions.

We have recently discovered the bis(Zn(II)-dipicolylamine (Dpa)) derivatives as the first artificial receptors for multiply phosphorylated peptides.¹⁰ Under neutral aqueous conditions, a binuclear Zn(II)-Dpa-bipyridyl derivative strongly ($K_{app} > 10^5 M^{-1}$) binds to bis-phosphorylated peptides via a two-point interaction, based on coordination chemistry between the Zn(II) sites and the phosphate groups (i.e., the cross-linking strategy). The preliminary results encouraged us to attempt the disruption of the phosphoprotein–protein interaction using the Zn(II)-Dpa complexes. Since the multiple phosphorylation serves as a common mechanism regulating protein function and constitutes a complicated regulatory program for signaling pathways like a dynamic “molecular barcode” in living cells,¹¹ it is expected that the targeting multiphosphorylated proteins by a synthetic small molecule will open a new possibility for artificial regulation of a signal transduction cascade. We now report that some of the artificial receptors can serve as a potent disruptor for the phosphoprotein–protein surface interaction via a cross-

Chart 1. Molecular Structure of the Artificial Receptors, and Amino Acid Sequences of the Pin1WW Domain (6–39) and the CTD Phosphopeptides Discussed Here



- (6) (a) Yin, H.; Hamilton, A. D. *Angew. Chem., Int. Ed.* **2005**, *44*, 4130. (b) Roy, B. C.; Banerjee, A. L.; Swanson, M.; Jia, X. G.; Haldar, M. K.; Mallik, S.; Srivastava, D. K. *J. Am. Chem. Soc.* **2004**, *126*, 13206. (c) Banerjee, A. L.; Swanson, M.; Roy, B. C.; Jia, X.; Haldar, M. K.; Mallik, S.; Srivastava, D. K. *J. Am. Chem. Soc.* **2005**, *126*, 10875. (d) Jain, R.; Ernst, J. T.; Kutzki, O.; Park, H. S.; Hamilton, A. D. *Mol. Diversity* **2004**, *8*, 89. (e) Salvatella, X.; Martinelli, M.; Gairi, M.; Mateu, M. G.; Feliz, M.; Hamilton, A. D.; de Mendoza, J.; Giralt, E. *Angew. Chem., Int. Ed.* **2004**, *43*, 196. (f) Gradl, S. N.; Felix, J. P.; Isacof, E. Y.; Garcia, M. L.; Trauner, D. *J. Am. Chem. Soc.* **2003**, *125*, 12668. (g) Fazal, M. A.; Roy, B. C.; Sun, S.; Mallik, S.; Rodgers, K. R. *J. Am. Chem. Soc.* **2001**, *123*, 6283. (h) Peczu, M. W.; Hamilton, A. D. *Chem. Rev.* **2000**, *100*, 2479.
- (7) (a) Ojida, A.; Miyahara, Y.; Kohira, T.; Hamachi, I. *Biopolymers (Peptide Science)* **2004**, *76*, 177. (b) Ojida, A.; Mito-oka, Y.; Sada, K.; Hamachi, I. *J. Am. Chem. Soc.* **2004**, *126*, 2454. (c) Ojida, A.; Mito-oka, Y.; Inoue, M.; Hamachi, I. *J. Am. Chem. Soc.* **2002**, *124*, 6256. (d) Mito-oka, Y.; Tsukiji, S.; Hiraoka, T.; Kasagi, N.; Shinkai, S.; Hamachi, I. *Tetrahedron Lett.* **2001**, *42*, 7059. (e) Takashima, H.; Shinkai, S.; Hamachi, I. *Chem. Commun.* **1999**, 2345.
- (8) (a) Baberjee, A. L.; Tobwala, S.; Haldar, M. K.; Swanson, M.; Roy, B. C.; Mallik, S.; Srivastava, D. K. *Chem. Commun.* **2005**, 2549. (b) Yin, H.; Lee, G.-I.; Sedey, K. A.; Kutzki, O.; Park, H. S.; Orner, B. P.; Ernst, J. T.; Wang, H.-G.; Sebtii, S. M.; Hamilton, A. D. *J. Am. Chem. Soc.* **2005**, *127*, 10191. (c) Yin, H.; Lee, G.-I.; Sedey, K. A.; Rodriguez, J. M.; Wang, H.-G.; Sebtii, S. M.; Hamilton, A. D. *J. Am. Chem. Soc.* **2005**, *127*, 5463. (d) Walensky, L. D.; Kung, A. L.; Escher, I.; Malia, T. J.; Barbuto, S.; Wright, R. D.; Wagner, G.; Verdine, G. L.; Korsmeyer, S. J. *Science* **2004**, *305*, 1466. (e) Arkin, M. R.; Wells, J. A. *Nat. Rev. Drug Discovery* **2004**, *3*, 301. (f) Berg, T. *ChemBioChem* **2004**, *5*, 1051. (g) Horswill, A. R.; Savinov, S. N.; Benkovic, S. J. *PNAS* **2004**, *44*, 15591. (h) Vassilev, L. T.; Vu, B. T.; Graves, B.; Carvajal, D.; Podlaski, F.; Filipovic, Z.; Kong, N.; Kammlot, U.; Lukacs, C.; Klein, C.; Fotouhi, N.; Liu, E. A. *Science* **2004**, *303*, 844. (i) Berg, T. *Angew. Chem., Int. Ed.* **2003**, *42*, 2462. (j) Cochran, A. G. *Curr. Opin. Chem. Biol.* **2001**, *5*, 654. (k) Cochran, A. G. *Chem. Biol.* **2000**, *7*, R85. (l) Blaskovich, M. A.; Lin, Q.; Delarue, F. L.; Sun, J.; Park, H. S.; Coppola, D.; Hamilton, A. D.; Sebtii, S. M. *Nat. Biotechnol.* **2000**, *18*, 1065.
- (9) (a) Song, Y.-L.; Roller, P. P.; Long, Y.-Q. *Bioorg. Med. Chem. Lett.* **2004**, *14*, 3205. (b) Sundaramoorthi, R.; Kawahata, N.; Yang, M. G.; Shakespeare, W. C.; Metcalf, C. A., III; Wang, Y.; Merry, T.; Eyer mann, C. J.; Bohacek, R. S.; Narula, S.; Dalgarno, D. C.; Sawyer, T. K. *Biopolymers (Peptide Science)* **2003**, *71*, 717. (c) Müller, G. *Top. Curr. Biol.* **2000**, *211*, 19. (d) Cody, W. L.; Lin, Z.; Panek, R. L.; Rose, D. W.; Rubin, J. R. *Curr. Pharm. Des.* **2000**, *6*, 59. (e) Nguyen, J. T.; Turck, C. W.; Cohen, F. E.; Zuckermann, R. N.; Lim, W. A. *Science* **1998**, *282*, 2088.
- (10) Ojida, A.; Inoue, M.; Mito-oka, Y.; Hamachi, I. *J. Am. Chem. Soc.* **2003**, *125*, 10184.
- (11) (a) Yang, X.-J. *Oncogene* **2005**, *24*, 1653. (b) Holmberg, C. I.; Tran, S. E. F.; Erikson, J. E.; Sistonon, L. *Trends Biochem. Sci.* **2002**, *27*, 619.

linking fashion. The detailed binding studies and the inhibition assay using the phosphorylated CTD peptide and the WW domain as a model pair revealed that the intramolecular juxtaposition of the two Zn(II)-Dpa sites at a suitable distance is crucial for the strong molecular recognition of the phosphorylated CTD peptide so as to produce the effective disruption for their surface interaction.

Results and Discussion

Molecular Design of BisZn(II)-Dpa as Disruptor for Phosphopeptide Interaction of WW Domain. WW domains are a small binding motif for the proline-rich sequence and found in many different signaling or structural proteins.^{2a,4d,12} They are composed of approximately 40 amino acids and folded as a stable, triple-stranded β -sheet. Among them, a WW domain derived from the peptidyl-prolyl isomerase Pin1 is a class IV WW domain, which specifically interacts with pSer-Pro or pThr-Pro motifs.¹³ In this study, a recognition pair of the Pin1 WW domain (6–39) and the CTD (C-terminal domain of RNA polymerase II) doubly phosphorylated peptide was employed as a model system for evaluating the inhibitory activity of our artificial receptors (Chart 1), because of the rich structural basis of their surface complex. An X-ray crystallographic analysis

- (12) (a) Sudol, M.; Sliwa, K.; Russo, T. *FEBS Lett.* **2001**, *490*, 190. (b) Zarrinpar, A.; Lim, W. A. *Nat. Struct. Biol.* **2000**, *7*, 611.
- (13) (a) Verdecia, M. A.; Bowman, M. E.; Lu, K. P.; Hunter, T.; Noel, J. P. *Nat. Struct. Biol.* **2000**, *7*, 639. (b) Xu, Y.-X.; Hirose, Y.; Zhou, X. Z.; Lu, K. P.; Manley, J. L. *Genes & Development* **2003**, *17*, 2765. (c) Lu, P.-J.; Zhou, X.-Z.; Liou, Y.-C.; Noel, J.-P.; Lu, K.-P. *J. Biol. Chem.* **2002**, *277*, 2381. (d) Wintjens, R.; Wieruszkeski, J.-M.; Drobeccq, H.; Rousselot-Pailley, P.; Buée, L.; Lippens, G.; Landrieu, I. *J. Biol. Chem.* **2001**, *276*, 25150.

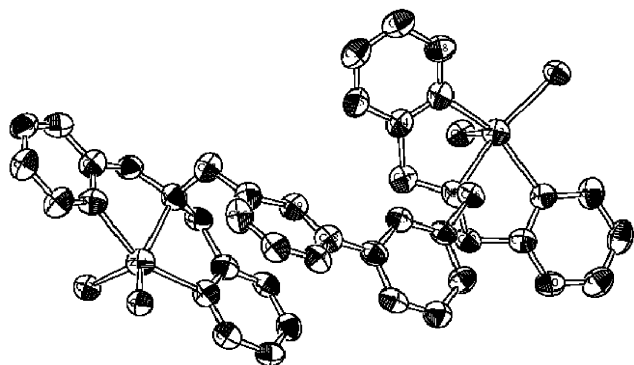


Figure 1. ORTEP drawing (50% probability ellipsoids) of the biphenyl compound **1** ($C_{38}H_{36}N_6 \cdot Zn_2Cl_4 \cdot Et_2O$). Hydrogen atoms and disordered solvent molecules are omitted for clarity.

of the complex of the Pin 1 WW domain with the doubly phosphorylated CTD peptide revealed that the phosphate group of the Ser9 of the CTD peptide tightly interacts with the Pin1 WW domain through the hydrogen bonding with the side chains of Ser16, Arg 17, and Tyr23 and the backbone amide of Arg17, whereas the phosphate group Ser6 does not participate in the specific binding. The complex structure also indicates that the distance of the two phosphate groups is 9.7 Å.^{13a}

To obtain a potent disruptor for the phosphopeptide/WW domain interaction using the cross-linking strategy, we prepared a family of binuclear Zn(II) complexes (**1–7**), which are designed to possess two Zn(II)-Dpa centers at a distinct distance by changing the spacer moiety (Chart 1). The receptor **5** possessing a phenyl group as the spacer has the shortest distance between the two Zn(II) centers (4–6 Å), whereas the longest one is **6** or **7** (14–17 Å), which possesses a 3,3'-styryl or terphenyl group as the spacer. The distance between the two Zn(II) centers is also adjustable by changing the substitution position of the Dpa sites on the biaryl spacer unit as shown in the biphenyl (**1** and **3**) and the bipyridyl types of artificial receptors (**2** and **4**). Among them, we successfully obtained the detail structural information about the biphenyl receptor of **1** by an X-ray crystallographic analysis (Figure 1). The binuclear Zn complex of **1** with Cl^- counterions crystallized from CH_3CN-Et_2O to afford a single crystal suitable for an X-ray analysis. It was revealed in the crystal state that the dihedral angle of the two phenyl groups of **1** is 37° and the distance of the two Zn(II) centers is 11.5 Å, which is relatively close to that of the two phosphate groups of the doubly phosphorylated CTD peptide (9.7 Å). Thus, it might be expected that the biphenyl type of receptor might be a potent inhibitor candidate for the phosphoprotein/WW domain interaction. All artificial receptors were prepared from the corresponding halomethyl compound by the substitution reaction with 2,2'-dipicolylamine and then by the metal complexation with $Zn(NO_3)_2$. As a monodentate control compound, the mononuclear receptor **8** was also prepared by the same procedure. The structures of these receptors were fully characterized by 1H NMR, mass spectroscopy, and elemental analysis (see Supporting Information).

Binding Studies between Artificial Receptor and Phosphorylated Peptide by Isothermal Titration Calorimetry. Prior to evaluating the inhibitory activity of these receptors, the binding affinity of the receptors with the phosphorylated peptides was quantitatively determined by isothermal titration calorimetry (ITC). Figure 2 shows the typical titration data of **1** with the

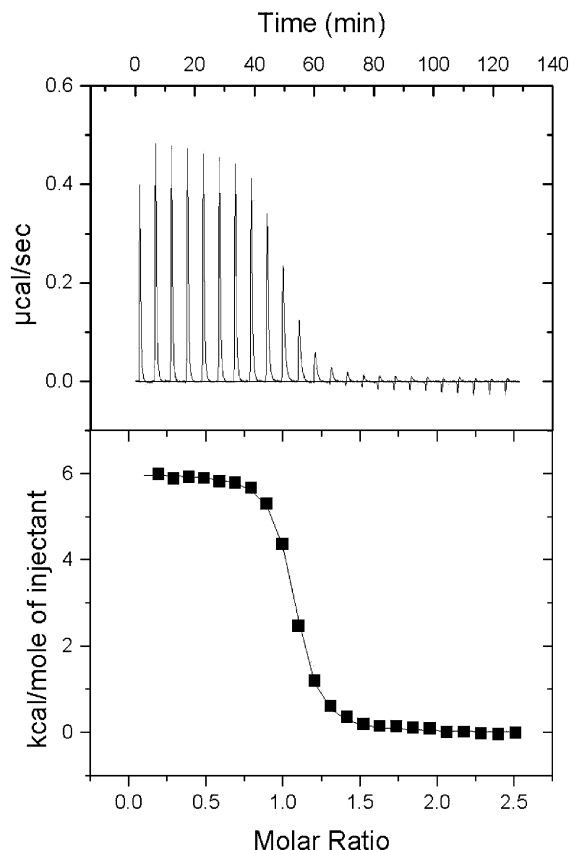


Figure 2. Typical ITC titration curve and processed data (for the titration of **1** with pS-6,9). Measurement conditions: $[1] = 20 \mu M$, $[pS-6,9] = 300 \mu M$ ($24 \times 10 \mu L$ injections), 50 mM HEPES buffer, pH 7.2, 25 °C.

doubly phosphorylated CTD fragment, pS-6,9 peptide. The resultant binding isotherm was fitted with a curve derived from the 1:1 binding algorithm ($n = 1.13$) to yield a binding constant of $(8.11 \pm 0.46) \times 10^6 M^{-1}$. Interestingly, the present interaction was an entropy-driven endothermic process ($\Delta S > 0$, $\Delta H > 0$), presumably due to the release of water molecules from the solvent sphere fixed around the receptor and/or the phosphopeptide. Table 1 summarized the thermodynamic parameters, as obtained by fitting the binding isotherm to a 1: n interaction model. Almost the same strong binding affinity was obtained in the case of the bipyridyl receptor **2** ($K = (2.80 \pm 0.36) \times 10^6 M^{-1}$, Table 1). The binding of **1** or **2** with the pS-6,9 peptide was much stronger than those of **8** with the pS-6,9 peptide or the singly phosphorylated pS-9 peptide, in which the binding affinities were estimated to be in the range of $10^3 M^{-1}$ by analyzing with a 1:2 binding model ($n = 0.5$) or with a 1:1 binding model ($n = 1.0$), respectively (Figure S1). These results suggest that **1** or **2** interacts with the pS-6,9 peptide via a two-point interaction so as to exhibit the remarkably strong binding affinity in aqueous solution. This is also supported by the ITC data between **1** and the pS-9 peptide, in which the slope of the titration curve was gentle even in the measurement with a relatively high concentration of **1** (100 μM), indicating that the binding with the pS-9 peptide is much weaker than that with the doubly phosphorylated pS-6,9 peptide (Figure S1).¹⁴ It is

(14) The rather largely deviated n value from 1 ($n = 1.35$) and the relatively large heat formation (7.89 kcal/mol) compared to the other bindings suggest that the complex formation between **1** and pS-9 peptide is not a single binding mode but a mixture of several binding modes containing a 1:2 or higher order complexes.

Table 1. Stoichiometry (n), Binding Constant (K , M^{-1}), Enthalpy (ΔH , $kcal\ mol^{-1}$), and Entropy ($T\Delta S$, $kcal\ mol^{-1}$) for the Interactions of the Artificial Receptors with the Phosphorylated Peptides^a

peptide		1	2	3	4	5	6	7	8
pS-6,9	n	1.14	0.99	0.69	0.70	1.00	0.57		0.50
	K	$(8.11 \pm 0.46) \times 10^6$	$(2.80 \pm 0.36) \times 10^6$			$(4.26 \pm 0.30) \times 10^5$		b	$(8.49 \pm 0.51) \times 10^3$
	ΔH	6.01 ± 0.02	4.53 ± 0.04	9.67 ± 0.23	6.79 ± 0.26	4.45 ± 0.05	9.34 ± 0.17		4.60 ± 0.12
	$T\Delta S$	1.54	13.3			12.2			9.95
pS-9	n	1.35				1.16			1.00
	K		b	b	b	$(4.24 \pm 0.42) \times 10^3$	b	b	$(1.11 \pm 0.11) \times 10^3$
	ΔH	7.89 ± 0.13				4.20 ± 0.66			3.09 ± 0.22
	$T\Delta S$					9.14			7.23

^a The thermodynamic parameters were obtained by fitting the binding isotherm to a 1: n interaction model, assuming a single type of binding mode. b Not measured.

to be noted that the strong binding of **1** or **2** with the pS-6,9 peptide is due to the favorable positive ΔS value that is significantly larger than those observed in the weak interactions of the mononuclear complex **8**. The large entropic gain of **1** or **2** observed here may be partially ascribed to the cooperativity of the two Zn(II)-Dpa sites in the binding to the pS-6,9 peptide.¹⁵ The ΔH value in the binding between **8** and the pS-9 peptide ((3.09 ± 0.22) kcal/mol) is almost half of that of the binding between **1** with the pS-6,9 peptide ($\Delta H = 6.01 \pm 0.02$ kcal/mol). In addition, the bindings between **2**, **5**, and **8** with the pS-6,9 peptide are also endothermic processes with 4.45–4.60 kcal/mol as a positive ΔH value.¹⁶ On the basis of these data, the average heat for the binding of a single Zn(II)-Dpa site per phosphate site is reasonably determined to be 2–3 kcal/mol. ITC experiments were also conducted for the other binuclear receptors **3**, **4**, and **6**, which have the two Zn(II) centers with different distances (Table 1). The rapid cease of the heat formation before the addition of 1 equiv of the pS-6,9 peptide gave the discrepancy in the 1:1 binding stoichiometry ($n = 0.57$ – 0.70), suggesting that the complex formation with **3**, **4**, or **6** is not 1:1 and may contain several different binding modes. In the case of the terphenyl derivative **7** that was not sufficiently soluble in water, we were not able to evaluate the binding property. These results imply that the strong affinity with the 1:1 binding with the doubly phosphorylated pS-6,9 peptide is achieved only in the case when the distance between the two Zn(II)-Dpa sites of the artificial receptor is suitable for the cross-linking interaction with the two phosphate groups. Since the distance of the two Zn(II) centers in **1** and **2** can be varied by the rotation of the biaryl unit, it may be reasonably assumed that they flexibly adjust the two Zn(II) distances to fit the distance between the two phosphate sites of the CTD peptide. On the other hand, such a flexible distance modulation does not operate for the corresponding para-substituted isomer **3** and **4**, resulting in the non-1:1 interaction.

Cross-Linking Binding Mode of Artificial Receptor with Phosphopeptide. The cross-linking binding mode of the receptors **1** or **2** with the phosphorylated peptides was explored by the circular dichroism (CD) studies. As shown in Figure 3a, the strong Cotton peaks at 200, 230, and 265 nm appeared in

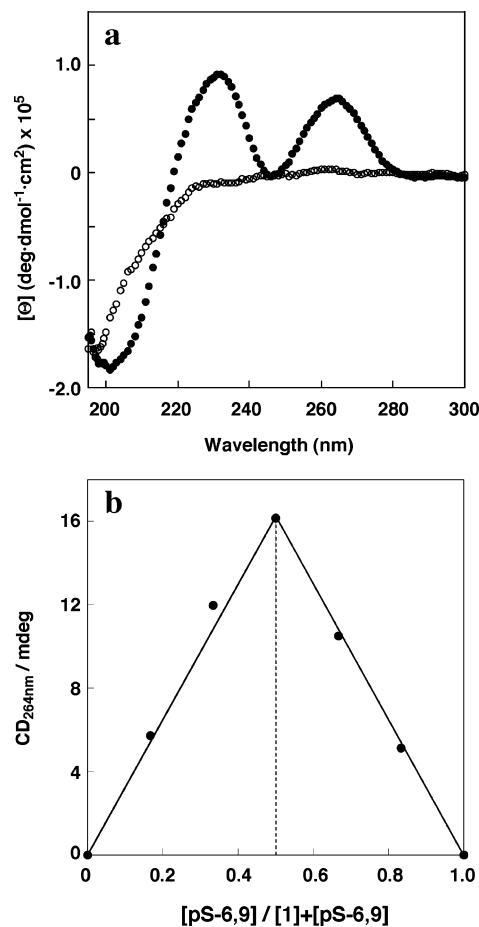


Figure 3. (a) CD spectra of the pS-6,9 peptide (20 μM) (○) and the complex between **1** (20 μM) and the pS-6,9 peptide (20 μM) (●). (b) CD Job titration between **1** and the pS-6,9 peptide, $[1] + [pS-6,9] = 40 \mu M$. Measurement conditions: 10 mM borate buffer, pH 8.0, 25 °C.

the complex **1** with the doubly phosphorylated pS-6,9 CTD peptide (20 μM in 10 mM borate buffer, pH 8.0). Similar strong Cotton peaks were also observed during the interaction with the bipyridyl receptor **2** (Figure S2). Since the peak maxima at 230 and 265 nm correspond to the absorption maxima of the receptor **1** or **2**, it is reasonably considered that the strong induced CDs are originated from the receptors by complexation with the pS-6,9 CTD peptide. On the other hand, no CD peaks were induced in the case of the interaction between the monophosphorylated pS-9 CTD peptide and **1** (data not shown). The induced CDs observed in the case of **1** or **2** upon the pS-6,9 peptide binding may reflect a chirally defined rigid

(15) (a) Tobey, S. L.; Anslyn, E. V. *J. Am. Chem. Soc.* **2003**, *125*, 10963. (b) Williams, D. H.; Westwell, M. S. *Chem. Soc. Rev.* **1998**, *27*, 57. (c) Jencks, W. P. *Proc. Natl. Acad. Sci. U.S.A.* **1981**, *78*, 4046.

(16) We previously revealed that the receptor **5** binds to a single phosphate group of a phosphopeptide using the two Dpa sites in a chelation-like fashion.⁷ However, the much stronger binding of **5** with the pS-6,9 peptide ($K = 4.26 \times 10^5 M^{-1}$) compared to that with the pS-9 peptide ($K = 4.24 \times 10^3 M^{-1}$) in the present case implies that **5** interacts with the two phosphate groups of pS-6,9 peptide with a cross-linking fashion like the binding mode of **1** or **2**.

conformation of the receptors via a two-point fixation within the complex with the pS-6,9 peptide. The job plot between **1** and the pS-6,9 peptide was also examined using the induced CD peak. The maximum CD change was observed when the molar ratio of **1** and the pS-6,9 peptide is equivalent, clearly indicating that the binding stoichiometry is 1:1 (Figure 3b). The 1:1 binding stoichiometry was also confirmed by the Job plot in the complex formation between **2** and the pS-6,9 peptide (Figure S2).

The two-point interaction of **1** with the pS-6,9 peptide is also supported by a ^{31}P NMR study. A broad single peak at 6.40 ppm corresponding to the two phosphate groups of pS-6,9 without **1** changed into the two separated and upfield shifted peaks at 4.53 and 3.68 ppm upon the addition of 1 equiv of **1** (Figure S3). The upfield shifts of the ^{31}P signal by complexation with the Zn(II)-Dpa complex was also observed in the case of the complexation with the 1,8-bisZn(II)-Dpa-anthracene compound as previously reported.^{3c} This result indicates that the cross-linking receptor **1** directly interacts with the two phosphate sites of the pS-6,9 peptide. In a ^1H NMR study, the four protons due to the C6 positions of the four pyridine rings of **1** were observed as a doublet at 8.50 ppm which is indistinguishable from each other, suggesting that **1** has a highly symmetrical structure in aqueous solution (Figure S4). However, this peak split into the four distinct peaks at 8.89, 8.78, 8.72, and 8.52 ppm upon addition of the pS-6,9 peptide. Other pyridine protons also changed into the different peaks in the complex with the pS-6,9 peptide. These results imply that the two Zn(II)-Dpa sites of **1** are involved in the interaction with the two phosphate sites of the pS-6,9 peptide so that four pyridine rings are located in the different environments.

Inhibitory Activity of Artificial Receptors Evaluated by Fluorescence Polarization Assay. The inhibitory activity of the artificial receptors toward the interaction between the Pin1 WW domain and the CTD peptide was evaluated by a fluorescence polarization assay using the rhodamine-labeled doubly phosphorylated peptide (Rho-pS-6,9). The fluorescence anisotropy value of Rho-pS-6,9 (50 mM HEPES, pH 7.2) increased to ~ 0.12 by the addition of the Pin1 WW domain, indicating the complex formation of Rho-pS-6,9 with the WW domain. The curve-fitting analysis of the obtained saturation curve afforded the affinity constant of $1.8 \times 10^5 \text{ M}^{-1}$ (Figure S5). When the receptor **1** was added to the solution containing the Pin 1 WW domain/Rho-pS-6,9 complex, a sharp decrease in the anisotropy value took place (Figure 4a). This change indicated that the receptor **1** releases Rho-pS-6,9 from the complex by the competitive displacement of the WW domain with **1**. A curve fitting analysis of the displacement titration gave the K_i value of **1** to be $1.84 \times 10^6 \text{ M}^{-1}$.¹⁷ The addition of the bipyridyl type receptor **2** also caused a sharp decrease in the anisotropy value like **1** ($K_i = 1.38 \times 10^6 \text{ M}^{-1}$, Figure S6), showing that both are effective disruptors for the interaction between the pS-6,9 CTD peptide and the WW domain. The displacement assay was also conducted for the monophosphorylated peptide (Rho-pS9), the affinity of which for the Pin1 WW domain ($K_{\text{app}} = 1.8 \times 10^5 \text{ M}^{-1}$) was comparable to the case of Rho-pS-6,9 (Figure S5). Interestingly, in this case, the anisotropy value did not decrease at all with the addition of **1**, indicating that **1** did not effectively inhibit the interaction of

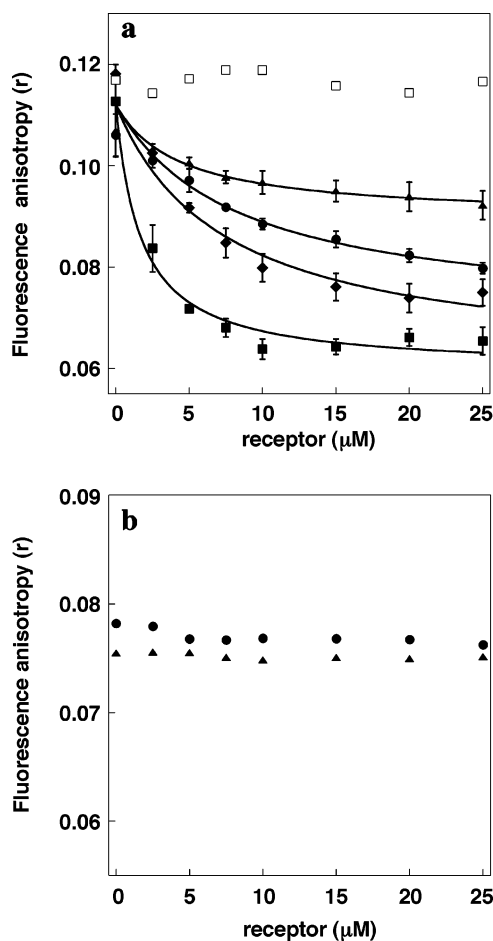


Figure 4. Fluorescent anisotropy change of the rhodamine-labeled phosphopeptide Rho-pS-6,9 ($5 \mu\text{M}$) upon the addition of the various artificial receptors (0 – $25 \mu\text{M}$) in the presence of the WW domain ($25 \mu\text{M}$). (a) pS-6,9 peptide with **1** (\blacksquare), **3** (\bullet), **5** (\blacktriangle), **6** (\blacklozenge), and **8** (\square). (b) pS-9 peptide with **1** (\blacktriangle) and **2** (\bullet). Measurement conditions: 50 mM HEPES buffer, pH 7.2, 20°C , $\lambda_{\text{ex}} = 550 \text{ nm}$.

the monophosphorylated peptide with the WW domain (Figure 4b). Such a sharp contrast suggests that the second phosphate site, which is not masked by the WW domain, is crucial for the effective disruption of the interaction. This is quite consistent with the ITC results, which shows the much weaker binding affinity of **1** with pS-9 rather than that with pS-6,9 (Table 1). As another control experiment, the mononuclear Zn(II) complex **8** was also used in the displacement assay for Rho-pS-6,9 (Figure 4a). As expected from the ITC result, **8** did not induce any anisotropy change. On the other hand, in the displacement assay using the receptors **3**–**6** (Figure 4a and Figure S6), which cannot form a tight 1:1 binding complex with the pS-6,9 peptide, the anisotropy value gently decreased upon addition of them, indicating that these receptors are moderate inhibitors, less potent than **1**. Thus, it can be concluded that the strong binding affinity due to the two-point metal–ligand interaction is essential for the effective disruption of the surface interaction of the WW domain with the phosphopeptide (Figure 5). It is noteworthy that the effective inhibition potency of **1** and **2** may enable us to propose that the direct and tight binding of the small artificial receptor to the phosphate group on a protein surface becomes an alternative promising strategy for the inhibition of the phosphoprotein–protein interaction.

(17) Kirk, S. R.; Luedtke, N. W.; Tor, Y. *J. Am. Chem. Soc.* **2000**, *122*, 980.

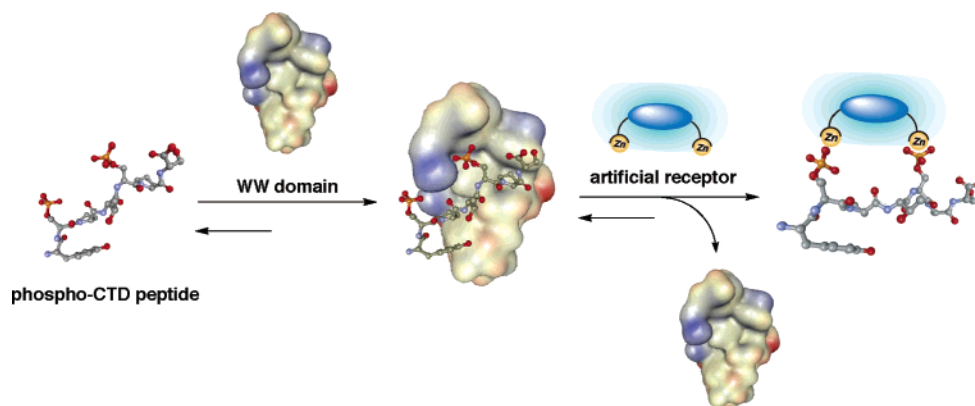


Figure 5. Schematic representation of the disruption of the phosphopeptide/WW domain interaction by the Zn(II) dipicolylamine-based artificial receptors.

Conclusion

We have demonstrated that the artificial receptors bearing the two Zn(II)-Dpa sites can strongly bind to the bis-phosphorylated peptide in a cross-linking manner under the neutral aqueous conditions, when the distance between the two Zn(II) centers can appropriately fit that of the two phosphate groups of the doubly phosphorylated peptide. On the basis of this finding, we have successfully carried out the effective disruption of the CTD phosphopeptide/Pin1 WW domain interaction using these types of small molecules. The cross-linking mode for inhibition by the artificial receptors presented herein, i.e., the selective recognition of a multiphosphorylated peptide depending on the number and the distance of the phosphate groups, should be a valuable strategy for disrupting other complexes involving various multiphosphorylated proteins. When the sufficient binding selectivity and affinity is acquired by combining a variety of interaction forces, this approach may lead to effective small molecular modulators or disruptors for signal cascades in living cells in future. We are currently evaluating this line of research.

Experimental Section

Synthesis of the Artificial Receptors. All zinc complexes (**1–8**) were synthesized from the corresponding halomethyl compound by the nucleophilic substitution with 2,2'-dipicolylamine and the subsequent zinc complexation. Characterizations of these compounds were performed by ^1H NMR, mass spectroscopy, and elemental analysis (see Supporting Information). Typical synthetic procedures are as follows:

3,3'-Bis[(2,2'-dipicolylamino)methyl]biphenyl. A solution of 3,3'-bis(bromomethyl)biphenyl¹⁸ (700 mg, 2.06 mmol), 2,2'-dipicolylamine (0.82 g, 4.12 mmol), and potassium carbonate (1.13 g, 8.23 mmol) in anhydrous DMF (10 mL) was stirred for 1.5 h at rt. After dilution with 1 N HCl, the resulting mixture was washed with AcOEt. The aqueous phase was alkalized with 2 N NaOH and extracted with AcOEt ($\times 2$). The combined organic layers were washed with water and brine followed by drying over MgSO_4 . After removal of the solvent in vacuo, the residue was purified by column chromatography (silica gel, $\text{CHCl}_3/\text{MeOH}/\text{NH}_3\text{aq} = 60/1/1$) to give the title compound (773 mg, 65%) as a pale yellow oil: ^1H NMR (400 MHz, CDCl_3) δ 3.77 (4H, s), 3.86 (8H, s), 7.17 (4H, t, $J = 6.0$ Hz), 7.37–7.46 (6H, m), 7.61–7.67 (10H, m), 8.52 (4H, d, $J = 4.8$ Hz). ^{13}C NMR (150 MHz, CDCl_3) δ 58.6, 60.1, 122.0, 122.8, 126.0, 127.6, 127.7, 128.7, 136.4, 139.5, 141.2, 149.0, 159.7. FAB-MS m/e 577.34 $[\text{M} + \text{H}]^+$.

3,3'-Bis[(2,2'-dipicolylamino)methyl]biphenyl 2Zn(NO₃)₂ Complex (1**).** To a solution of 3,3'-bis[(2,2'-dipicolylamino)methyl]biphenyl (201 mg, 0.35 mmol) in CH_3CN (2 mL) was added dropwise an aqueous solution of 0.596 M $\text{Zn}(\text{NO}_3)_2$ (1.05 mL, 0.63 mmol), and the mixture was stirred for 30 min at rt. After removal of the solvent in vacuo, the residue was diluted with distilled H_2O , filtered through a cellulose acetate filter (pore size 0.45 μm), and lyophilized. The obtained solid was filtered and washed with AcOEt to give the Zn(II) complex (220 mg, 66%) as a colorless powder: ^1H NMR (400 MHz, D_2O) δ 3.77 (4H, s), 3.87 (4H, d, $J = 15.6$ Hz), 4.27 (4H, d, $J = 16.0$ Hz), 7.15 (4H, d, $J = 8.0$ Hz), 7.43–7.47 (6H, m), 7.50–7.56 (6H, m), 7.95 (4H, t, $J = 7.6$ Hz), 8.59 (4H, d, $J = 4.8$ Hz). ^{13}C NMR (150 MHz, $\text{D}_2\text{O} + \text{CD}_3\text{OD}$) δ 56.8, 56.9, 126.0, 126.4, 128.8, 130.9, 131.1, 132.0, 133.4, 142.3, 142.6, 149.4, 155.8. FAB-MS m/e 893.15 $[\text{M} - \text{NO}_3]^+$. Anal. Calcd for $\text{C}_{38}\text{H}_{36}\text{N}_6 \cdot 2\text{Zn}(\text{NO}_3)_2$: C, 47.76; H, 3.80; N, 14.66. Found: C, 47.42; H, 3.75; N, 14.25.

Peptide Synthesis. The peptide coupling was performed with an automated peptide synthesizer (ABI 433A, Applied Biosystems). Purification of peptide was carried out with a Hitachi L-7100 HPLC system. The molecular weight of the peptide was confirmed by mass spectrometer (MALDI-TOF, Perseptive Biosystems Voyager DE-RP) using 3,5-dimethoxy-4-hydroxycinnamic acid as a matrix.

(i) Synthesis of Pin1 WW Domain. The Pin1 WW domain (6–39) was synthesized using the standard Fmoc-based FastMoc coupling chemistry (0.25 mmol scale) on Alko-PEG Resin preloaded with Fmoc-Glycine (0.1 mmol, loading rate: ~ 0.22 mmol/g, purchased from Watanabe Chemical Industries, Ltd.). The coupling reactions were performed using 10 equiv of amino acid and 10 equiv of 1-hydroxybenzotriazole (HOBt). The peptide cleavage from resin and side-chain deprotection were carried out by treatment with 10 mL of TFA containing *m*-cresol (0.25 mL), thioanisole (0.75 mL), and ethanedithiol (0.75 mL) over 1 h at rt. After removal of TFA in vacuo, the crude peptide was precipitated in cold diethyl ether and purified by reversed-phase HPLC (column; YMC-pack ODS-A, 20 Φ \times 250 mm). Purification conditions were as follows: mobile phase, CH_3CN (0.1% TFA)/ H_2O (0.1% TFA) = 23/77 \rightarrow 30/70 (linear gradient over 40 min); flow rate, 9.9 mL/min; detection, UV (220 nm). MALDI-TOF mass: calcd for $[\text{M} + \text{H}]^+$ 4025.1, found 4024.6.

(ii) Synthesis of Phosphopeptide. The peptides were synthesized using the standard Fmoc-based FastMoc coupling chemistry (0.1 mmol scale) on Fmoc-Amide Resin (Applied Biosystems). Fmoc-Ser[PO(O Obz)OH]-OH (Watanabe Chemical Industries, Ltd.) was used as a phosphorylated amino acid unit for the peptide coupling. The peptide cleavage from resin and side-chain deprotection were carried out by the treatment with TFA–*m*-cresol–thioanisole (86:2:12) over 1 h at rt. After removal of TFA in vacuo, the crude peptide was precipitated in *tert*-butyl-methyl ether and purified by reversed-phase HPLC (column; YMC-pack ODS-A, 20 Φ \times 250 mm). Purification

(18) Tashiro, M.; Yamato, T. *J. Org. Chem.* **1985**, *50*, 2939.

conditions were as follows: mobile phase, CH₃CN (0.1% TFA)/H₂O (0.1% TFA) = 5/95 → 24/76 (linear gradient over 25 min); flow rate, 9.9 mL/min; detection, UV (220 nm). MALDI-TOF mass pS-6,9: calcd for C₄₇H₇₀N₁₂O₂₅P₂ [M - H]⁻ 1265.1, found 1265.8; pS-9: calcd for C₄₇H₇₁N₁₂O₂₂P [M - H]⁻ 1187.1, found 1186.1.

(iii) Synthesis of Rhodamine-Conjugated Peptide. A purified phosphopeptide, tetramethylrhodamine isothiocyanate (2 equiv, a mixture of 5-, 6-isomer purchased from Molecular Probes, Inc.), and diisopropylethylamine (4 equiv) were dissolved in DMF, and the mixture was stirred 5 h at rt. After completion of the reaction (checked by HPLC analysis), the obtained peptide was purified by HPLC (column; Desovil ODS-UG-5, 10Φ × 250 mm). Purification conditions were as follows: mobile phase, CH₃CN/100 mM AcNH₄ in H₂O = 15/85 → 40/60 (linear gradient over 40 min); flow rate, 3 mL/min; detection, UV (220 nm). MALDI-TOF mass: calcd for C₇₂H₉₀N₁₄O₂₉P₂S [M - H]⁻ 1708.6, found 1711.23.

X-ray Crystallography. X-ray diffraction data were collected on a Rigaku R-AXIS RAPID diffractometer with a 2D area detector using graphite-monochromatized Cu K radiation ($\lambda = 1.5418 \text{ \AA}$) at ca. 120 K. Lattice parameters were obtained by least-squares analysis from reflections for three oscillation images. Direct methods (SIR92) were used for the structure solution. All calculations were performed using the TEXSAN¹⁹ crystallographic software package. All non-hydrogen atoms are found by Fourier syntheses. The structure was refined by a full matrix least-squares procedure using observed reflections ($> 2.0 \sigma(I)$) based on F^2 , and all non-hydrogen atoms were refined with anisotropic displacement parameters and hydrogen atoms were placed in idealized positions with isotropic displacement parameters relative to the connected non-hydrogen atoms and not refined. Crystallographic parameters are summarized in the Supporting Information.

Isothermal Titration Calorimetry (ITC). ITC titration was performed on an Isothermal Titration Calorimeter from MicroCal Inc. All measurements were conducted at 298 K. In general, a solution of the peptide (1–2 mM) in 50 mM HEPES buffer (pH 7.2) was injected stepwise (10 $\mu\text{L} \times 24$) to a solution of the artificial receptor (20–100 μM) dissolved in the same solvent system. The concentration of the phosphorylated peptide was determined based on the UV absorbance of the tyrosine residue ($\epsilon = 1530 \text{ M}^{-1} \text{ cm}^{-1}$ at 274 nm²⁰). The measured heat flow was recorded as a function of time and converted into enthalpies (ΔH) by integration of the appropriate reaction peaks. Dilution effects were corrected by subtracting the results of a blank experiment with a solution of 50 mM HEPES solution (pH 7.2) in place of peptide solution under the identical experimental conditions. The binding parameters (K_{app} , ΔH , ΔS , n) were evaluated by applying a one-site model using the software Origin (MicroCal Inc.).

Circular Dichroism (CD). CD spectra were recorded using a JASCO J-720W spectropolarimeter. The aqueous solution of the phosphopeptide (20 μM) in 10 mM borate buffer (pH 8.0) in the absence and the presence of the artificial receptor (20 μM) was prepared, and CD spectra of the solutions were measured from 340 to 200 nm (scan speed; 50 nm/min) at 4 °C using a water-jacketed quartz cell (1 mm path length). Each spectrum represents the average of 16 time scans

with smoothing to reduce noise. In a Job plot, a titration of continuous variation was conducted where the concentration of both the receptor **1** or **2** and the pS-6,9 peptide was varied between 0 and 40 μM such that the number of moles in solution stayed constant.

Nuclear Magnetic Resonance (NMR). ³¹P NMR spectra were recorded on a Bruker DRX-600 (243 MHz) at 25 ± 1 °C. 85% H₃PO₄ was used as an external reference. Samples were prepared using a concentration of 0.5 mM pS-6,9 peptide in 50 mM HEPES (pH 7.2)/D₂O (90:10) in the absence and presence of 0.5 mM receptor **1**.

¹H NMR spectra were recorded on a JEOL JNM A-400 (400 MHz) at 25 ± 1 °C. Samples were prepared using a concentration of 0.5 mM of **1** in D₂O in the absence and presence of 0.5 mM of the pS-6,9 peptide. The observed peaks were individually assigned by the COSY experiments.

Fluorescence Anisotropy Experiment. Fluorescence anisotropy experiments were performed with a Perkin-Elmer LS55 spectrometer. A stock solution of the artificial receptor (1–2 mM in distilled H₂O) was titrated into an aqueous solution (0.5 mL) containing the rhodamine-conjugated peptide (5 μM) and the Pin1 WW domain (25 μM) in 50 mM HEPES (pH 7.2). The fluorescence emission of the rhodamine-conjugated peptide (Rho-pS-6,9 or Rho-pS-9) was measured ($\lambda_{\text{ex}} = 550 \text{ nm}$) at 20 °C upon titration of the receptors, and the fluorescence anisotropy value (r) was calculated using the emission intensity at 576 nm by eq 1,²¹

$$r = \frac{I_V - G \cdot I_H}{I_V + 2G \cdot I_H} \quad (1)$$

where I_V and I_H are the fluorescence intensities observed through polarizers parallel and perpendicular to the polarization of the exciting light, respectively, and G is a correction factor accounting for instrumental differences in the fluorescence detection. Experimental data were fitted into eq 2 to determine the IC₅₀ value, which was in turn used to determine the K_i value (M^{-1}) according to the reported method,¹⁷

$$r = \frac{X \cdot r_{\text{min}} + r_{\text{max}} \cdot \text{IC}_{50}}{X + \text{IC}_{50}} \quad (2)$$

where X is the concentration of the artificial receptor.

Acknowledgment. M.I. thanks JSPS for his JSPS predoctoral fellowship. This work is partially supported by the Nagase Science Foundation.

Supporting Information Available: Synthesis and characterization of the artificial receptors, selected crystallographic parameters for **1**, selected data of the ITC experiments, experimental data of the CD study of **2**, ³¹P and ¹H NMR studies of **1** and the pS-6,9 peptide, and selected data of the fluorescent anisotropy experiments (PDF); X-ray crystallographic data of **1** (CIF). This material is available free of charge via the Internet at <http://pubs.acs.org>.

JA056585K

(21) Weber, G. *Adv. Protein Chem.* **1953**, *8*, 415.

(19) TEXAN, X-ray structure analysis package; Molecular Structure Corp.: The Woodland, TX, 1985.

(20) Nishio, H.; Kosaka, A.; Hembury, G. A.; Matsushima, K.; Inoue, Y. *J. Chem. Soc., Perkin Trans.* **2002**, 582.